Desalination and Water Treatment
www.deswater.com

doi:10.5004/dwt.2018.22725

124 (2018) 287–296
August

Pomegranate peels collected from fresh juice shop as a renewable precursor for high surface area activated carbon with potential application for methylene blue adsorption

Ali H. Jawad[a,*], Muna Hasoon Sauodi[b], Mohd Sufri Mastuli[a], Mohammed Ajah Aouda[c], Khairul Adzfa Radzun[a]

[a]*Faculty of Applied Sciences, Universiti Teknologi MARA, 40450 Shah Alam, Selangor, MALAYSIA, Tel. +60355211721, email: ahjm72@gmail.com, ali288@salam.uitm.edu.my (A.H. Jawad), Tel. + 60355436594, email: mohdsufri@salam.uitm.edu.my (M.S. Mastuli), Tel. +603 5543 6594, email: khairuladzfa@salam.uitm.edu.my (K.A. Radzun)*
[b]*Chemistry Department, College of Science, Al-Muthanna University, Al-Muthanna, IRAQ, Tel. +9647834406070, email: munaforever2004@gmail.com (M.H. Sauodi)*
[c]*Chemistry Department, College of Science, Thi-Qar University, Thi-Qar, IRAQ, Tel. +9647801420155, email: Mohaja2009@yahoo.com (M.A. Aouda)*

Received 29 July 2017; Accepted 7 July 2018

ABSTRACT

Pomegranate (*Punica Granatum*) peels were utilized as precursors to prepare mesoporous activated carbon (PPAC) *via* H_3PO_4-activation method. The surface characterization of PPAC was achieved using Fourier Transform Infrared (FTIR), Scanning Electron Microscopy (SEM), N_2 adsorption/desorption, X-Ray Diffraction (XRD), and the point of zero charge (pH_{PZC}) method. It was found that PPAC a large surface area and total pore volume corresponded to 1280.45 m^2/g and 1.343 cm^3/g, respectively. The adsorption properties of PPAC with methylene blue (MB) was conducted at different adsorbent dose (0.2–3 g/L), solution pH (3–11), initial dye concentrations (50 mg/L–400 mg/L), contact time (0–135 min) using batch mode operation. The kinetic uptake profiles are well described by the pseudo-second-order model, while the Langmuir model describes the adsorption behaviour at equilibrium. The maximum adsorption capacity of PPAC with methylene blue was 384.61 mg/g at 303 K. Various thermodynamic parameters such as standard enthalpy ($\Delta H°$), standard entropy ($\Delta S°$) and standard free energy ($\Delta G°$) showed that the adsorption of MB onto PPAC was favourable and endothermic in nature.

Keywords: Pomegranate peel; Activated carbon; Adsorption; Methylene blue; Phosphoric acid

1. Introduction

Effluents generated from dyeing industries, such as textile and printing, have been identified as emerging environmental problems in aquatic environments. Most of these dyes are highly visible, stable and resistant to chemical, photochemical as well as biological degradation. Besides, they are often toxic and carcinogenic due to their complex aromatic structure and synthetic nature [1]. Basic dyes are cationic species charged sites that reside on heteroatoms such as nitrogen or sulfur atoms. Such basic dye species present an obvious coloration even at low concentration (<1 mg/L) and are classified as toxic colorants [2]. Methylene blue (MB) is a basic dye with favourable water solubility that is used in industrial activities such as dyeing of textiles and leather, printing calico, printing cotton, and biological staining methods [3]. The acute exposure to MB dye may cause eye irritation, gastrointestinal irritation and nausea upon ingestion, including vomiting and diarrhea [4].

*Corresponding author.

Adsorption is among the most efficient, simple and inexpensive techniques for the removal of dye effluents [5]. In this case, activated carbon (AC) is a widely used adsorbent due to its large surface area, high adsorption capacity and various surface functional groups [6]. Carbonaceous materials from natural or synthetic sources can be used to produce AC. Alternatively, the production of carbon-based adsorbents from agricultural wastes represents an interesting design strategy because the precursors are cheap, renewable, safe, abundance and readily available [7].

Recently, agricultural waste peels have been recognized as an ecological burden for the society. However, waste peels, as lignocellulosic biomass-rich materials, have stimulated new gateways for the production of renewable, low cost and sustainable adsorbents for water treatment applications. Moreover, fruits and vegetables wastes and by-products, which are formed in great amounts during industrial processing, represent a serious problem, as they exert an influence on environment and need to be managed and/or utilized [8]. Therefore, researchers have studied the production of ACs from fruit and vegetable peels as cheap and renewable precursors, such as jackfruit peel [9], mangosteen peel [10], pineapple peel [11], Citrus fruit peel [12], potato peel [13], rambutan peel [14], pomegranate peel [15], grapefruit peel [16], cassava peel [17], *Cucumis sativus* peel [18], pomelo peel [19], banana peel [20], guava peel [21], mandarin peel [22], and mango peel [23].

Pomegranate (*Punica Granatum*) is one of the famous fruit in the world due to its delicious taste as well as rich with nutrition. It consists of edible part, seed, and peel. Pomegranate peel (PP) is a by-product from pomegranate juice, hence it can be considered as waste which owns no commercial value. It was found that the PP constitutes from 5 to 15% of its total weight [24]. In fact, PP is a natural, eco-friendly and low-cost precursors of activated carbon (AC), which can be utilized in the removal of diverse types of aquatic pollutants and also reduce pollution. Being a renewable resource, PP can be considered as a promising precursor for producing high quality activated carbon suitable for environmental technology if applied in the treatment of water and wastewaters.

In particular, the main objective of this work is to develop a high surface area AC from Pomegranate peels (PPAC) by using H_3PO_4-activation method. Among the numerous activating agents used for chemical activation, H_3PO_4 has been commonly used due to environmental and economic concerns. The structural characterization of PPAC was performed using gas adsorption, scanning electron microscopy (SEM) and Fourier transform infrared (FTIR), and elemental analyzer (CHN). The physicochemical parameters were evaluated such as iodine number and point of zero charge (pH_{PZC}). The role of porous structure of PPAC in adsorption process of selected MB as the model adsorbate at variable adsorbent dosage, pH, initial dye concentration and contact time for this unique biomaterial is considered.

2. Materials and methods

2.1. Materials

The pomegranate peels (PP) were obtained from a local fresh juice shop in Shah Alam, Selangor, Malaysia. Phosphoric acid (H_3PO_4; Hmbg Chemicals) was used as the chemical reagent for activation of the coconut leaves. Methylene Blue (MB) was obtained from R & M Chemicals with the following properties; chemical formula ($C_{16}H_{18}ClN_3S_3H_2O$), molecular weight (373.9 g/mol), and solubility in water (40 g/L). Other chemicals such as potassium hydroxide (KOH), hydrochloric acid (HCl), sodium hydroxide (NaOH), iodine, sodium thiosulphate, potassium bromide and sodium chloride were of analytical grade and used as received unless specified otherwise.

2.2. Preparation of PPAC

The pomegranate peels based activated carbon (PPAC) was prepared by predetermined optimum impregnation ratio of H_3PO_4: biomass (1:3 wt. %) with occasional stringing, and then kept in an oven for 24 h at 110°C. The sample was then placed in a stainless steel vertical tubular reactor and put in the furnace. The carbonization process was conducted under high purified nitrogen gas (99.99%) with 450°C under the pressure of 1 atm for 1 h. The activated products were then cooled to room temperature and washed with 3 M of HCl solution followed by hot distilled water until the filtrate turn neutral pH (~pH 7). The PPAC was then dried in an oven at 110°C for 24 h. After that, the PPAC was ground and the powder was sieved to obtain a particle size range of 212 µm–350 µm. Finally the PPAC was stored in tightly closed bottles for subsequent use. The yield of the activated carbon was calculated by the following equation:

$$Yield(\%) = \frac{Wt.\ of\ PPAC}{Wt.\ of\ dried\ PP} \times 100 \quad (1)$$

2.3. Characterization of PPAC

Nitrogen adsorption–desorption experiment was carried out by BET Sorptometer, BET-201A analyzer at 77 K. Specific surface area was determined by BET method, the total pore volume was calculated by nitrogen adsorption at $p/p^\circ = 0.995$, and pore size distribution was determined from the adsorption branch with Barrett–Joyner–Halenda (BJH) theory. The scanning electron microscope (SEM) images of the samples were obtained using a JEOL USA Scanning Electron Microscopes. Infrared spectra of the adsorbents were obtained using a Fourier transform infrared spectrometer at room temperature in the 4000–500 cm^{-1} wavenumber range (Perkin Elimer, Spectrum One, FT-IR Spectrometer). For the FT-IR analysis, finely ground adsorbent has been intimately mixed with KBr (Merck) in a ratio of 1:100 in order to prepare a translucent pellet. Ultimate analyses of the samples were measured for determining C, H, N, and S content by CHNS-O Analyzer (Flash 2000, Organic Elemental Analyzer, Thermo-scientific). The oxygen contents were calculated by difference. X-ray diffraction analysis (XRD) was performed on coal in order to determine the crystallinity or amorphous nature before and after activating process by X-ray diffraction (XRD) in reflection mode (Cu Kα radiation) on a PANalytical, X'Pert Pro X-ray diffractometer. Scans were recorded with a scanning rate of 0.59°/s. The diffraction angle (2θ) was varied from 10°

to 90°. The surface physical morphology was examined by using scanning electron microscopy (SEM-EDX) technique. The samples were placed on carbon tapes, and then coated with a thin layer of gold–palladium in an argon atmosphere using Agar Sputter Coater. The iodine number indicates the porosity of the activated carbon and it is defined as the amount of iodine adsorbed by 1 g of carbon at the mg level, which was determined by standard method [26]. Bulk or apparent density was determined according to the Lubrizol Standard Test Method [27].

2.4. Batch adsorption experiments

The batch adsorption experiments of MB onto PPAC were performed in a series of 250 mL Erlenmeyer flasks containing 100 mL of MB solution. The flasks were capped and agitated in an isothermal water bath shaker (Memmert, waterbath, model WNB7-45, Germany) at a fixed shaking speed of 90 strokes/min and 30°C until equilibrium was achieved. Batch adsorption experiments were carried out on common variables of interest such as adsorbent dosage (0.02–0.3 g), pH (3–10), initial dye concentration (50–400 mg/L) and contact time (0–135 min) to determine the optimum conditions for dye sorption. The pH of MB solution was adjusted by adding either 0.10 M HCl or NaOH to the desired pH value by monitoring with a pH meter (Metrohm, Model 827 pH Lab, Switzerland). After the stirring, the supernatant was collected with a 0.20 μm Nylon syringe filter and the concentrations of MB were monitored at a different time interval using a HACH DR 2800 Direct Reading Spectrophotometer at a wavelength of 661 nm.

The adsorption capacity at equilibrium, q_e (mg/g) and the percent of color removal, *CR* (%) of MB were calculated using Eqs. (2) and (3) respectively.

$$q_e = \frac{(C_o - C_e)V}{W} \tag{2}$$

$$CR\,\% = \frac{(C_o - C_e)}{C_o} \times 100 \tag{3}$$

where C_0 is the initial dye concentration (mg/L); C_e is the dye concentration at equilibrium (mg/L); V is the volume of dye solution used (mL); and W is the dry mass of the adsorbent used (g). Adsorption experiments were conducted in triplicate and are reported as average values.

3. Results and discussion

3.1. Physicochemical properties of PPAC

The measured physicochemical properties of PPAC are summarized in Table 1 where it is seen that PPAC has a reasonable yield of carbon (25.8%) and also high carbon content (74.34) as indicated by elemental analysis. Moreover, PPAC has a relatively low bulk density, ash content and moisture content. This observation indicates that PPAC has high carbon porosity, low mineral content or inorganic residue with low water content. On the other hand, PPAC has a good iodine number and its value is higher than the reported value for AC prepared from coconut leaves by H_3PO_4 activation [25]. On the other hand, PPAC has a large Brunauer–Emmett–Teller (BET) surface area (1280.46 m^2/g), which is in good agreement with results for mesoporous AC materials obtained from iodine number test.

Table 1
Physicochemical characteristics of PPAC

Typical properties	
Bulk density (g/mL)	0.11
Iodine number (mg/g)	1209
BET surface area (m^2/g)	1280.46 m^2/g
Proximate analysis (wt. %)	
Ash content	4.18
Moisture content	6.64
Fixed carbon (yield)	25.8
Ultimate analysis (wt. %)	
C	74.34
H	1.17
N	0.17
S	Not detected
O (by difference)	24.32

3.2. Characterization of PPAC

Fig. 1 shows the N_2 adsorption/desorption isotherm of PPAC at 77 K with the corresponding pore-size distribution (PSD). Based on the International Union of Pure and Applied Chemistry (IUPAC) classification, the isotherm profile belongs to the combination of type I and type II isotherms [28]. The combined features of both types of isotherm are attributed to the presence of micropore and mesopore structure. Based on plotted graph, isotherm profile belongs to the type IV. Type IV isotherm is given by many mesoporous industrial adsorbents and this type indicates the multilayer formation at low pressure after monolayer coverage. The International Union of Pure and Applied Chemistry (IUPAC) defines the pores based on their pore diameter as micropores (<20 Å), mesopores (20–500 Å) and macropores (>500 Å) [28]. The pore-size distribution shown in Fig. 1b reveals the mesopore character of PPAC.

XRD pattern of the PPAC is shown in Fig. 2. XRD pattern shows a broad hump indicating that PPAC is amorphous in nature. However, a second hump around 400 indicates that there exists a short-range crystallographic ordering in the sample. No sharp peaks, indicative of any crystalline phase, can be observed from the XRD pattern.

The SEM micrographs of PPAC samples before and after MB adsorption are shown in Figs. 3a and 3b, respectively. The SEM image reveals that the surface of PPAC before adsorption (Fig. 3a) is highly heterogeneous. Pores with different size and shape are also clearly visible. The pores are generated due to the evaporative loss of the activator from the AC surface during the activation process. In fact, the role of H_3PO_4 is to induce widening of microporosity of biomass, and leads to an increase in the volume of micropores, with all pore sizes being developed in a common proportion, thus leading to activated carbons with different volumes of micropores but with the same

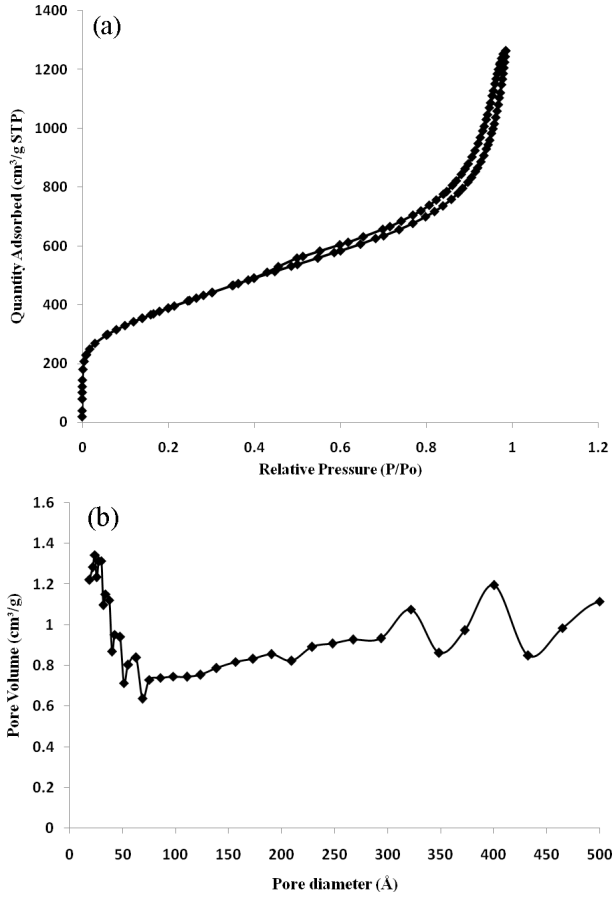

Fig. 1. Isotherms of N_2 adsorption–desorption (a) and pore size distribution (b) for PPAC.

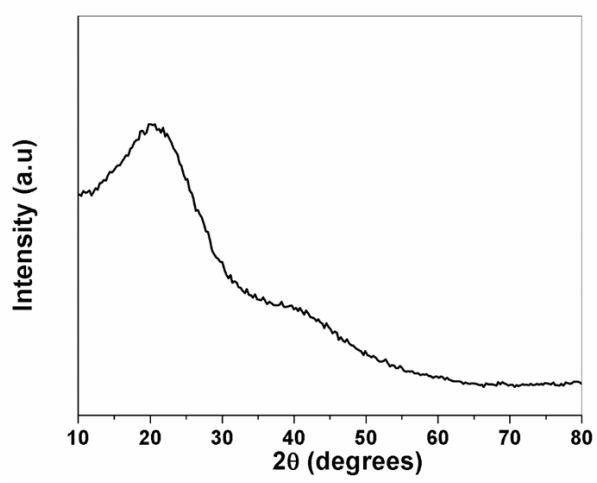

Fig. 2. XRD pattern of PPAC.

micropore size distribution [29]. The resulting pore structure is suitable for the adsorption of MB within the pore structure of PPAC. This assumption is supported by Fig. 3b where the PPAC surface is altered after MB adsorption as evidenced by more dense and less open pores are seen on the surface of PPAC.

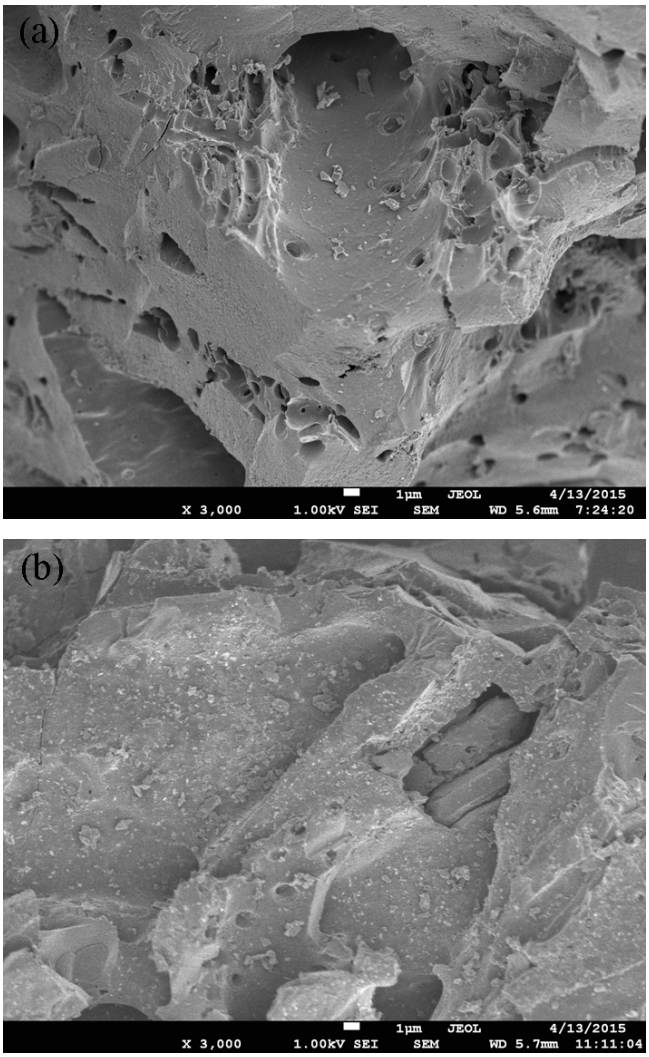

Fig. 3. SEM images of PPAC (a) before adsorption and (b) after MB adsorption at magnification power (3.00 KX).

The FT-IR spectrum of PPAC before MB adsorption shows that various bands are observed in Fig. 4a. The band at 3400 cm^{-1} is attributed to the hydroxyl (–OH) groups, which indicate the presence of carboxyl, phenol or alcohol groups on the surface of PPAC [30]. The weak band observed from 3000 to 2800 cm^{-1} is assigned to the aliphatic C–H stretching (methine, methyl and methylene groups of side chains) and from aromatic C–H stretching near 3100 cm^{-1}. The band at about at 1600–1580 cm^{-1} is assigned to C=C vibrations in aromatic rings. The peak at ~1200 cm^{-1} can be assigned to P=OOH groups from phosphates, and to the vibration of O–C in the P-O-C aromatic [31]. The band at ~1100–1000 cm^{-1} can be ascribed to P^{+}–O^{-} in acid phosphate esters [32]. The bands at 800–400 cm^{-1} can be ascribed to the carboxylate, alkane, secondary cyclic alcohol, and alkene groups. After MB adsorption, new IR bands appear and many functional groups are undergone red or blue shifting (Fig. 4b). New bands assigned to anhydride at ~16850 and nitro (~1300 cm^{-1}) are attributed to MB molecules loaded onto PPAC surface.

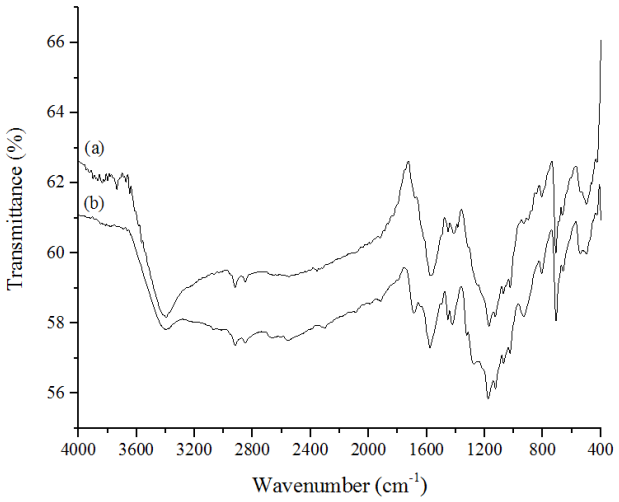

Fig. 4. FTIR spectra of PPAC (a) before adsorption and (b) after MB adsorption.

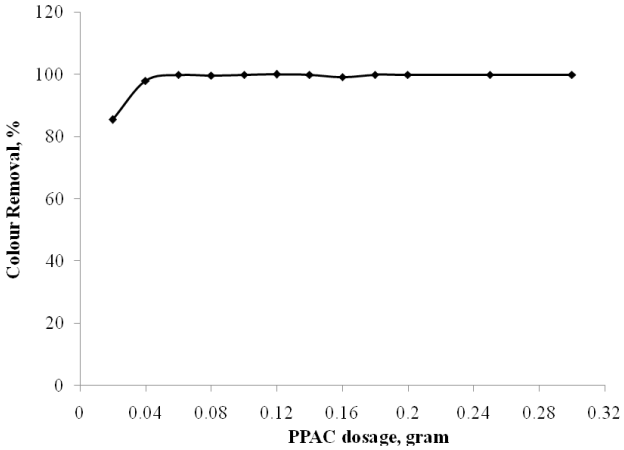

Fig. 5. Effect of adsorbent dosage on the percent removal and amount of adsorbed MB onto PPAC ($[MB]_o$ = 100 mg/L, Temp. = 303 K, contact time 60 min, and unadjusted pH of solution 5.60).

3.3. Batch adsorption studies

3.3.1. Effect of adsorbent dosage

The quantity of the available sorbent in the liquid phase is an important parameter that strongly affects sorption capacity. Variable dosage amounts of PPAC (0.02–0.3 g) were added to the 100 mL MB solution. The effect of PPAC dosage on MB removal is shown in Fig. 5. It is apparent that by increasing the PPAC dosage from 0.02 to 0.06 g, the percentage of MB removal increased from 85.4% to 99.8%. The increase in the MB removal by increasing PPAC dosage was due to the increase in the surface area of available PPAC in solution. A higher adsorbent dosage also reflects a greater the number of active adsorption sites available [33]. Therefore, 0.06 g/100 mL was selected for further adsorption studies.

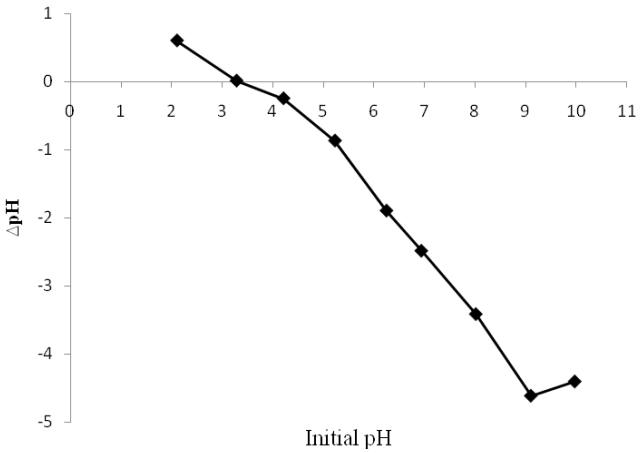

Fig. 6. pH_{PZC} of PPAC suspensions.

3.3.2. Effect of pH

The pHpzc is the pH where the adsorbent net surface charge corresponds to zero, and it offers the possible mechanism about the electrostatic interaction between adsorbent and adsorbate [34]. The pHpzc value of 3.2 was obtained for PPAC as shown in Fig. 6. Moreover, Fig. 7 shows the effect of pH, which ranged from 3 to 11, on MB uptake by PPAC at an initial MB concentration of 100 mg/L. The surface of PPAC is negatively charged at the pH ~3.2 and above. When the pH is increased from 3 to 11, the surface of PPAC may adopt negative surface charge which enhances adsorption of positively charged MB cations through attractive electrostatic attractions, contributing to an increase in the rate of adsorption [35]. Therefore, the MB adsorption efficiency was not affected by pH within the range due to buffering effect of the adsorbent [36]. Similar observations have been reported for the adsorption of methylene blue onto surface of activated carbon developed from coconut leaves by H_3PO_4activation [25], and KOH activation [37]. Thus, the pH value of unadjusted MB solution (pH 5.6) was used for further investigations.

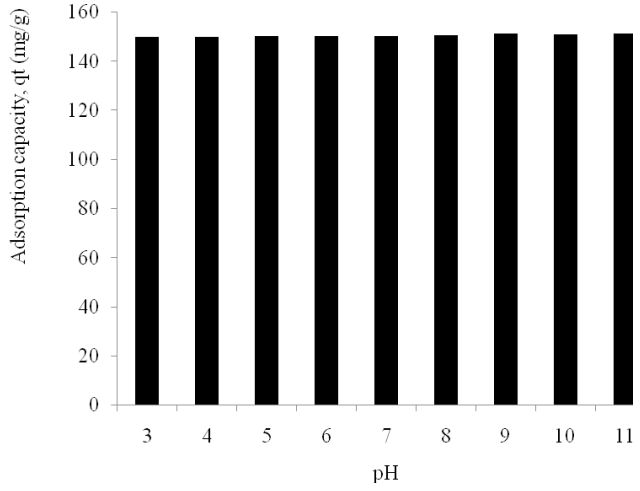

Fig. 7. Effect of solution pH on the percent removal of MB onto PPAC [MB initial concentration = 100 mg/L, Temp. = 303 K, contact time 60 min, and mass of PPAC 0.06 g/100 mL].

3.3.3. Effect of initial dye concentration and contact time

The influence of contact time and initial MB concentration (50–400 mg/L) on the adsorption capacity of PPAC are shown in Fig. 8. It was observed that the increase in initial MB concentration from 25 to 400 mg/L resulted in rapid increase in the uptake of MB by PPAC at equilibrium from 88.20 to 386.54 mg/g, respectively. This could be attributed to the increased collision rate between MB cations and PPAC surface by increasing the initial MB concentration. Furthermore, the time to reach equilibrium also increased with the increase in initial MB concentration as the MB shows the tendency to move deeper from the surface of PPAC to get attached to the more active adsorption sites.

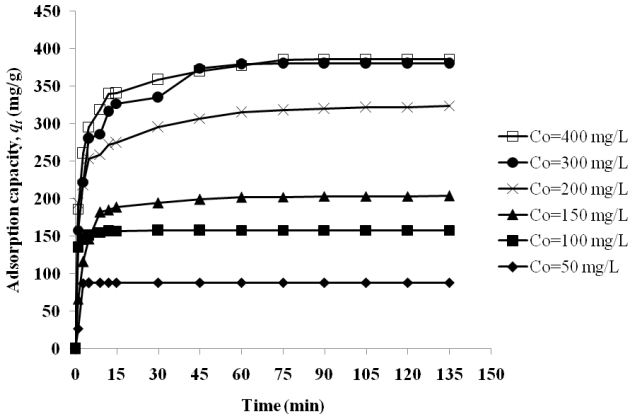

Fig. 8. Effect of initial dye concentrations and contact time on the uptake of MB onto PPAC [pH = 5.80, Temp. = 303 K, and mass of PPAC 0.06 g/100 mL].

3.4. Isotherm modeling

The adsorption equilibrium was evaluated using Langmuir and Freundlich isotherms. Langmuir isotherm is probably the most widely applied isotherm model in many adsorption studies. The model was developed based on assumptions that adsorption occurs at specific homogeneous sites on the adsorbent [38], and was used successfully in many monolayer adsorption processes. It also assumes no transmigration of adsorbate in the plane of adsorbent surface. The non-linear and linear Langmuir equations can be written as Eqs. (4) and (5), respectively:

$$q_e = \frac{q_{\max} K_a C_e}{1 + K_a C_e} \text{ (Non-linear form)} \quad (4)$$

$$\frac{C_e}{q_e} = \frac{1}{q_m K_L} + \frac{1}{q_m} C_e \text{ (Linear from)} \quad (5)$$

where $q_{\max}$ (mg/g) is the maximum adsorption capacity and b (L/mg) is a constant related to energy of adsorption which quantitatively reflects the affinity between the adsorbent and adsorbate. Therefore, a plot of C_e/q_e versus C_e gives a straight line of slope $1/q_{max}$ and intercept $1/(q_{max}K_L)$. The both non-linear and liner Langmuir plots are shown in Fig. 9, and their corresponding isotherm values are recorded in Table 2. Conversely, the Freundlich is an empirical equation proposed by Freundlich [39] to describe the sorption behavior of solute concentration on heterogeneous surface. The nonlinear and linear equations of the Freundlich model can be expressed by the following Eqs. (6) and (7) respectively.

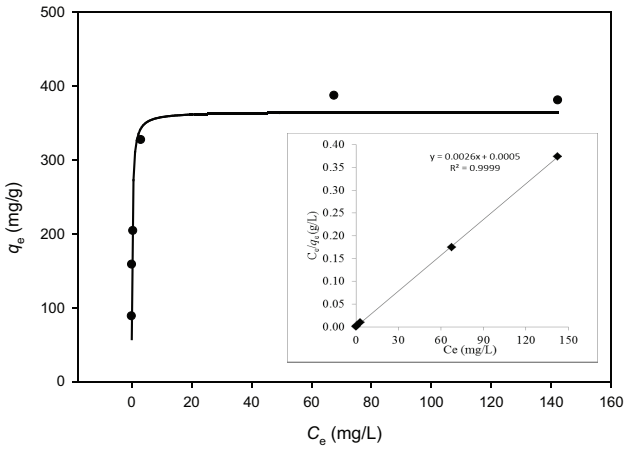

Fig. 9. Adsorption isotherm plots of the non-linear and linear Langmuir models for MB adsorption on PPAC at 303 K.

$$q_e = K_f C_e^{1/n} \text{ Non-linear form} \quad (6)$$

$$\ln q_e = \ln K_F + \frac{1}{n} \ln C_e \text{ Linear from} \quad (7)$$

where K_F (mg/g) represents adsorption capacity and n is related to adsorption intensity (unitless). A plot of ln q_e versus ln C_e will give a straight line of slope $1/n$ and intercept K_F. The both non-linear and liner Freundlich plots are shown in Fig. 10, and their corresponding isotherm values are recorded in Table 2. After analyzing the parameter values of the isotherms presented in Table 2, the R^2 value was close to unity, indicating isotherm data fitted well to the Langmuir plot. The results suggest that the adsorption takes place on homogeneous sites that are energetically equivalent [40]. Thus, PPAC shows relatively high adsorption capacity for

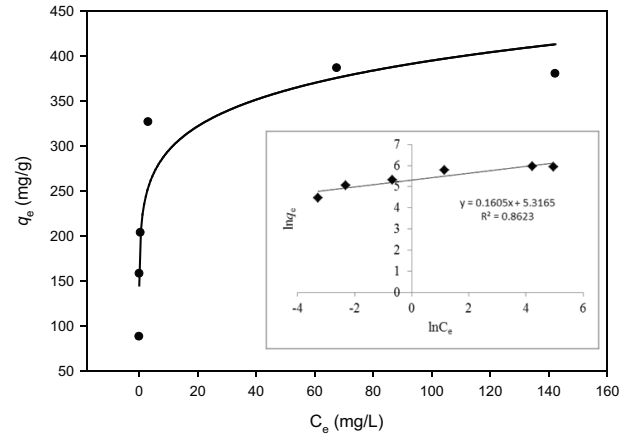

Fig. 10. Adsorption isotherm plots of the non-linear and linear Freundlich models for MB adsorption on PPAC at 303 K.

MB, where q_m was 384.61 mg/g, exceeding values reported for other types of AC materials prepared by using H_3PO_4 activation from various available precursors for the uptake of MB as listed in Table 3. Therefore, the PPAC produced in this study is an effective adsorbent and represents a viable precursor for the production of AC adsorbent materials.

3.5 Adsorption kinetics

The kinetic data were analyzed using two different kinetic models namely: pseudo-first-order (PFO) model and pseudo-second-order (PSO) model. The PFO model was proposed initially by Lagergren and Svenska [45] and its linearized form is expressed by Eq. (8) as follows:

$$\ln(q_e - q_t) = \ln q_e - k_1 t \quad (8)$$

where q_e(mg/g) and q_t (mg/g) are the amount of MB adsorbed by PPAC at equilibrium and time t, respectively; while k_1 (1/min) is the PFO model rate constant.

The values of k_1 and $q_{e,cal}$ can be estimated from the slope and intercept of $\ln(q_e - q_t)$ vs. t, respectively as shown in Fig. 11a. The linear form of the PSO model [46] is described by Eq. (9):

$$\frac{t}{q_t} = \frac{1}{k_2 q_e^2} + \frac{t}{q_e} \quad (9)$$

where k_2(g/(mg·min)) is the PSO rate constant. The values of k_2 and $q_{e,cal}$ were calculated from the intercept and slope

Table 2
Parameters of the Langmuir and Freundlich isotherm models for MB adsorption on PPAC surface at 303 K

Langmuir isotherm		
q_m (mg/g)	K_L (L/mg)	R^2
Non-linear		
364.75	4.97	0.9133
Linear		
384.61	5.2	0.999
Freundlich isotherm		
K_F ((mg/g) (L/mg)$^{1/n}$)	$1/n$	R^2
Non-linear		
220.12	7.88	0.8757
Linear		
14.45	0.16	0.862

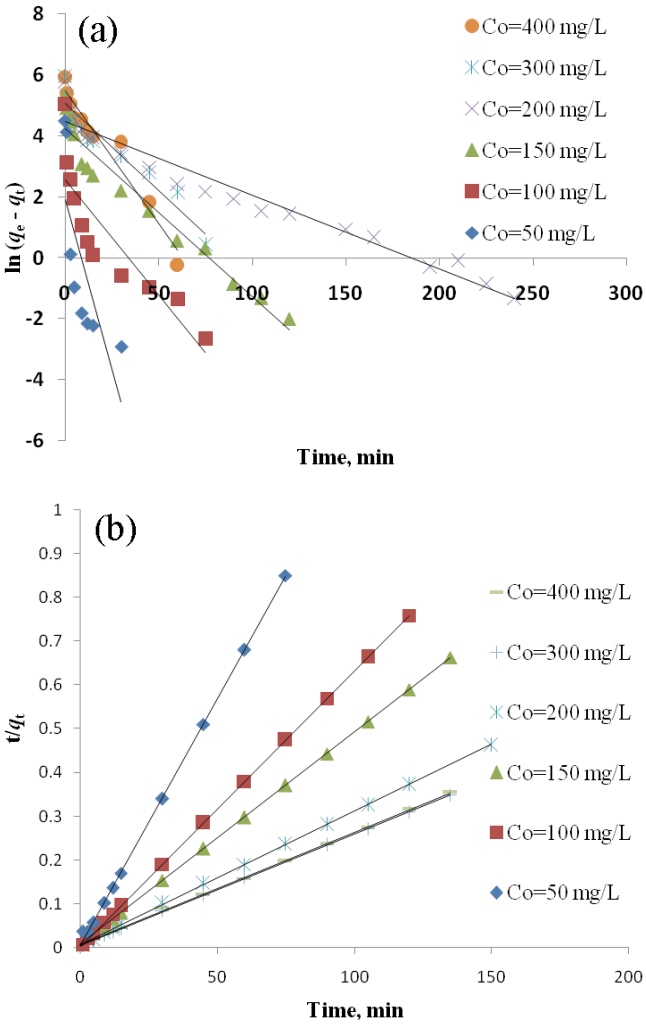

Fig. 11. Kinetic profiles for the adsorption of MB onto PPAC at 303K: (a) pseudo-first-order and (b) pseudo-second-order.

Table 3
Comparison of adsorption capacities for MB onto different activated carbons prepared by H_3PO_4 activation

Precursor	BET surface area (m^2/g)	Activating conditions	Dosage	pH	Temp. K	Adsorption capacity (mg/g)	References
Pomegranate peel	1280.45	Conventional heating	0.6 g/L	5.6	303	364.75	This work
Coconut leaves	981	Conventional heating	0.6 g/L	5.6	303	357.14	[25]
Coconut leaves	631.6	Microwave heating	2 g/L	5.6	303	250	[6]
Cotton cake	584	Conventional heating	2 g/L	7	302	250	[41]
Cotton stalk	652	Microwave heating	4 g/ L	7	298	245.7	[42]
Bamboo	1335	Microwave heating	1 g/L	–	298	183.3	[43]
Rice straw	522	Conventional heating	0.2–2 g/L	–	303	109.1	[44]

Table 4
PFO and PSO kinetic parameters and their corresponding values at different initial dye concentration by PPAC

Parameters	Initial dye concentration (mg/L)					
	50	100	150	200	300	400
$q_{e,exp}$ (mg/g)	88.200	158.130	203.615	326.573	386.541	380.282
Pseudo-first-order						
$q_{e,cal}$ (mg/g)	6.707	12.935	68.416	86.904	146.369	238.126
k_1 (1/m)	0.2205	0.0756	0.0549	0.0242	0.0510	0.0868
R^2	0.563	0.764	0.948	0.956	0.927	0.941
Pseudo-second-order						
$q_{e,cal}$ (mg/g)	89.285	158.730	208.330	333.330	400.000	384.615
k_2 (g/mg min)	0.023	0.033	0.003	0.001	0.001	0.001
R^2	0.993	1.000	1.000	1.000	0.999	1.000

of t/q_t versus t, respectively. The plotted graph is shown in Fig. 11b. The kinetic parameters of the two models are shown Table 4 along with its linear regression coefficients, R^2, where R^2 values are favourable ($R^2 \geq 0.99$) for the PSO model. Furthermore, the values of $q_{e.cal}$ are in agreement with the experimental values ($q_{e,exp}$). Therefore, the PSO model shows a better fit relative to the PFO model for kinetic uptake properties of MB onto PPAC.

3.6. Thermodynamics modeling

Adsorption functions such as Gibbs free energy (ΔG°), enthalpy (ΔH°) and entropy (ΔS°) provide important information about the mechanism and adsorption behavior of an isothermal system. The values of these thermodynamic functions were determined according to the following equations at 303, 313, 323, and 333 K [47]:

$$\ln K_d = \frac{\Delta S^\circ}{R} - \frac{\Delta H^\circ}{RT} \quad (10)$$

$$\Delta G^\circ = -RT \ln K_d \quad (11)$$

where R (8.314 J/mol K) is the universal gas constant, T (K) is the absolute solution temperature, and K_d (L/mg) is the distribution coefficient which can be calculated following equation:

$$K_d = \frac{q_e}{C_e} \quad (12)$$

where q_e (mg/g) is the equilibrium concentration of MB molecules on the activated carbon surface, and C_e (mg/L) is the is the equilibrium concentration of MB molecules in the solution. The values of ΔH° and ΔS° were calculated from the slope and intercept of van't Hoff plots ($\ln K_d$ versus $1/T$) as shown in Fig. 12, and the corresponding data are listed in Table 5.

The ΔG° values for the adsorption of MB adsorption at various temperatures (303, 313, 323 and 333 K) are recorded as –18.22, –18.15, –18.08 and –18.01 kJ/mol, respectively. The negative values of ΔG° revealed favorably and spontaneous nature of adsorption with high preference of MB molecules onto PPAC. Meanwhile, the determined ΔH° value was –60.24 kJ/mol, the negative value of ΔH° shows an exothermic nature of adsorption for the PPAC. The positive value of ΔS° (136.63 J/(mol·K)) shows that the affinity of PPAC to MB and its randomness at the solid/solution interface increases during the adsorption process [48].

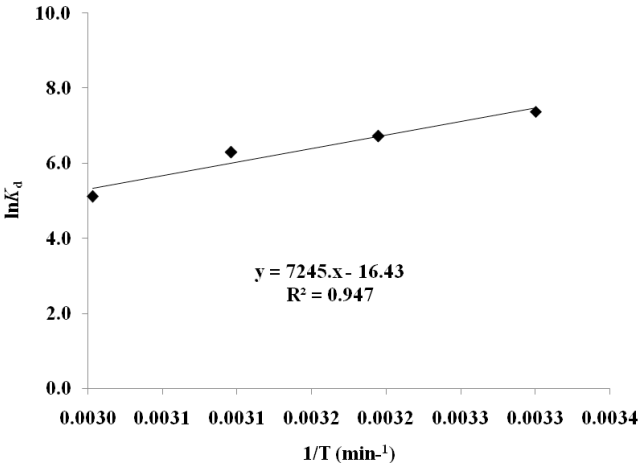

Fig. 12. Plot of $\ln k_d$ vs. 1/T for estimation of thermodynamic parameters for the adsorption of MB onto PPAC ($[MB]_o$ = 100 mg/L, V = 100 mL, pH = 5.6, and mass of PPAC 0.06 g/100 mL).

Table 5
Thermodynamic parameters values for the adsorption of MB onto PPAC

Temperature (K)	Thermodynamics Parameters			
	k_d	ΔG° (kJ/mol)	ΔH° (kJ/mol)	ΔS° (J/mol K)
303	1602.57	–18.22	–60.24	136.63
313	832.41	–18.15		
323	542.83	–18.08		
333	166.66	–18.01		

4. Conclusions

Pomegranate (*Punica Granatum*) peel was utilized as a low-cost precursor for preparation of a large surface area activated carbon (PPAC). Additionally, the surface area and iodine number of PPAC were 1280.46 m^2/g and 1209 mg/g, respectively. The prepared PPAC shows efficient removal for MB from aqueous solution. In this study, Equilibrium adsorption data of MB onto PPAC was well represented by Langmuir isotherm model, showing maximum adsorption capacity of 384.61 mg/g. The adsorption kinetic data were well described by the pseudo-second order model. Thus, these results indicated that PPAC is a low-cost and an efficient adsorbent for MB adsorption.

Acknowledgments

The authors would like to thank AL-Muthanna University in IRAQ for supporting this research work under International Research Grant (100-IRMI/INT 16/6/2 (001/2018)).

References

[1] N.S.A. Mubarak, A.H. Jawad, W.I. Nawawi, Equilibrium, kinetic and thermodynamic studies of Reactive Red 120 dye adsorption by chitosan beads from aqueous solution, Energ. Ecol. Environ., 2 (2017) 85–93.
[2] A.H. Jawad, A.F.M. Alkarkhi, N.S.A. Mubarak, Photocatalytic decolorization of methylene blue by an immobilized TiO_2 film under visible light irradiation: Optimization using response surface methodology (RSM), Desal. Water Treat., 56 (2015) 161–172.
[3] A.H. Jawad, N.S.A. Mubarak, M.A.M. Ishak, K. Ismail, W.I. Nawawi, Kinetics of photocatalytic decolourization of cationic dye using porous TiO_2 film, J. Taibah Univ. Sci., 10 (2016) 352–362.
[4] A.H. Jawad, R.A. Rashid, R.M.A. Mahmuod, M.A.M. Ishak, N.N. Kasim, K. Ismail, Adsorption of methylene blue onto coconut (Cocos nucifera) leaf: optimization, isotherm and kinetic studies, Desal. Water Treat., 57 (2016) 8839–8853.
[5] A.H. Jawad, M.A. Islam, B.H. Hameed, Cross-linked chitosan thin film coated onto glass plate as an effective adsorbent for adsorption of reactive orange 16, Int. J. Biol. Macromolec., 95 (2017) 743–749.
[6] A.H. Jawad, S. Sabar, M.A.M. Ishak, L.D. Wilson, S.S.A. Norrahma, M.K. Talari, A.M. Farhan, Microwave-assisted preparation of mesoporous activated carbon from coconut (Cocos nucifera) leaf by H_3PO_4-activation for methylene blue adsorption, Chem. Eng. Commun., 204 (2017) 1143–1156.
[7] M.J. Ahmed, S.K. Theydan, Physical and chemical characteristics of activated carbon prepared by pyrolysis of chemically treated date stones and its ability to adsorb organics, Powder Technol., 229 (2012) 237–245.
[8] A. Bhatnagar, M. Sillanpää, A. Witek-Krowiak, Agricultural waste peels as versatile biomass for water purification – A review, Chem. Eng. J., 270 (2015) 244–271.
[9] K.Y. Foo, B.H. Hameed, Potential of jackfruit peel as precursor for activated carbon prepared by microwave induced NaOH activation, Bioresour. Technol., 112 (2012) 143–150.
[10] K.Y. Foo, B.H. Hameed, Factors affecting the carbon yield and adsorption capability of the mangosteen peel activated carbon prepared by microwave assisted K_2CO_3 activation, Chem. Eng. J., 180 (2012) 66–74.
[11] K.Y. Foo, B.H. Hameed, Porous structure and adsorptive properties of pineapple peel based activated carbons prepared via microwave assisted KOH and K_2CO_3 activation, Microporous Mesoporous Mater., 148 (2012) 191–195.
[12] S. Dutta, A. Bhattacharyya, A. Ganguly, S. Gupta, S. Basu, Application of response surface methodology for preparation of low-cost adsorbent from citrus fruit peel and for removal of methylene blue, Desalination, 275 (2011) 26–36.
[13] A.C. Arampatzidou, E.A. Deliyanni, Comparison of activation media and pyrolysis temperature for activated carbons development by pyrolysis of potato peels for effective adsorption of endocrine disruptor bisphenol-A, J. Colloid Interface Sci., 466 (2016) 101–112.
[14] V.O. Njoku, K.Y. Foo, M. Asif, B.H. Hameed, Preparation of activated carbons from rambutan (*Nephelium lappaceum*) peel by microwave-induced KOH activation for acid yellow 17 dye adsorption, Chem. Eng. J., 250 (2014) 198–204.
[15] M.A. Ahmad, N.A.A. Puad, O.S. Bello, Kinetic, equilibrium and thermodynamic studies of synthetic dye removal using pomegranate peel activated carbon prepared by microwave-induced KOH activation, Water Resour. Ind., 6 (2014) 18–35.
[16] Y.Y. Pei, J.Y. Liu, Adsorption of Pb^{2+} in wastewater using adsorbent derived from grapefruit peel, Adv. Mater. Res., 391–392 (2011) 968–972.
[17] H.I. Owamah, Biosorptive removal of Pb(II) and Cu(II) from wastewater using activated carbon from cassava peels, J. Mater. Cycles Waste Manage., 16 (2014) 347–358.
[18] R. Pandey, N.G. Ansari, R.L. Prasad, R.C. Murthy, Removal of Cd(II) ions from simulated wastewater by HCl modified *Cucumis sativus* peel: equilibrium and kinetic study, Air Soil Water Res., 7 (2014) 93–101.
[19] O.S. Bello, M.A. Ahmad, B. Semire, Scavenging malachite green dye from aqueous solutions using pomelo (*Citrus grandis*) peels: kinetic, equilibrium and thermodynamic studies, Desal. Water Treat., 56 (2015) 521–535.
[20] K. Amela, M.A. Hassen, D. Kerroum, Isotherm and kinetics study of biosorption of cationic dye onto banana peel, Energy Procedia., 19 (2012) 286–295.
[21] P. Singh, P. Raizada, D. Pathania, G. Sharma, P. Sharma, Microwave induced KOH activation of guava peel carbon as an adsorbent for congo red dye removal from aqueous phase, Indian J. Chem. Technol., 20 (2013) 305–311.
[22] D.Z. Husein, Adsorption and removal of mercury ions from aqueous solution using raw and chemically modified Egyptian mandarin peel, Desal. Water Treat., 51 (2013) 6761–6769.
[23] A.H. Jawad, N.F.H. Mamat, M. Fauzi, K. Ismail, Adsorption of methylene blue onto acid-treated mango peels: kinetic, equilibrium and thermodynamic study, Desal. Water Treat., 59 (2017) 210–219.
[24] M.R. Moghadam, N. Nasirizadeh, Z. Dashti E. Babanezhad, Removal of Fe (II) from aqueous solution using pomegranate peel carbon: equilibrium and kinetic studies, Intern. J. Indust. Chem., 4 (2013) 19.
[25] A.H. Jawad, R.A. Rashid, K. Ismail, S. Sabar, High surface area mesoporous activated carbon developed from coconut leaf by chemical activation with H_3PO_4 for adsorption of methylene blue, Desal. Water Treat., 74 (2017) 326–335.
[26] Lubrizol standard test method, Iodine value, test procedure AATM 1112-01, October 16, 2006.
[27] M. Ahmedna, W.E. Marshall, R.M. Rao, S.J. Clarke, Use of filtration and buffers in raw sugar colour measurements, J. Sci. Food Agric., 75 (1997) 109–116.
[28] K.S.W. Sing, D.H. Everett, R.A.W. Haul, L. Moscou, R.A. Pierotti, J. Rouquérol, T. Siemieniewska, Reporting physisorption data for gas/solid systems with special reference to the determination of surface area and porosity, Pure Appl. Chem., 57 (1985) 603–619.
[29] M. Molina-Sabio, F. Rodriguez-Reinoso, Role of chemical activation in the development of carbon porosity, Colloids. Surf. A Physicochem. Eng. Asp., 241 (2004) 15–25.
[30] M.D. Pavlović, A.V. Buntić, K.R. Mihajlovski, S.S. Šiler-Marinković, D.G. Antonović, Ž. Radovanović, S.I. Dimitrijević-Branković, Rapid cationic dye adsorption on polyphenol-extracted coffee grounds—a response surface methodology approach, J. Taiwan Inst. Chem. Eng., 45 (2014) 1691–1699.

[31] J. Xu, L. Chena, H. Qua, Y. Jiaoa, J. Xie, Preparation and characterization of activated carbon from reedy grass leaves by chemical activation with H_3PO_4, Appl. Sur. Sci., 320 (2014) 674–680.
[32] A.M. Puziy, O. I. Poddubnaya, A. Martínez-Alonso, A. Castro-Muniz, F. Suárez-García, J.M.D. Tascón, Oxygen and phosphorus enriched carbons from lignocellulosic material, Carbon, 45 (2007) 1941–1950.
[33] B. Hayati, N.M. Mahmoodi, Modification of activated carbon by the alkaline treatment to remove the dyes from wastewater: mechanism, isotherm and kinetic, Desal. Water Treat., 47 (2012) 322–333.
[34] M.A. Islam, M.J. Ahmed, W.A. Khanday, M. Asif, B.H. Hameed, Mesoporous activated carbon prepared from NaOH activation of rattan (*Lacosperma secundiflorum*) hydrochar for methylene blue removal, Ecotoxicol. Environ. Saf., 138 (2017) 279–285.
[35] S. Chakraborty, S. Chowdhury, P. Das Saha, Adsorption of crystal violet from aqueous solution onto NaOH-modified rice husk, Carbohydr. Polym., 86(4) (2011) 1533–1541.
[36] K.C. Bedin, A.C. Martins, A.L. Cazetta, O. Pezoti, V.C. Almeida, KOH-activated carbon prepared from sucrose spherical carbon: adsorption equilibrium, kinetic and thermodynamic studies for Methylene Blue removal, Chem. Eng. J., 286 (2015) 476–484.
[37] R.A. Rashid, A.H. Jawad, M.A.M. Ishak, N.N. Kasim, KOH-activated carbon developed from biomass waste: adsorption equilibrium, kinetic and thermodynamic studies for Methylene blue uptake, Desal. Water Treat., 57 (2016) 27226–27236.
[38] I. Langmuir, The adsorption of gases on plane surfaces of glass, mica and platinum, J. Am. Chem. Soc., 40 (1918) 1361–1403.
[39] H. Freundlich, Ueber die adsorption in Loesungen (Adsorption in solution), Z. Phys. Chem., 57 (1906) 385–470.
[40] K.Y. Foo, B.H. Hameed, B.H. Preparation, characterization and evaluation of adsorptive properties of orange peel based activated carbon via microwave induced K_2CO_3 activation, Bioresour. Technol., 104 (2012) 679–686.
[41] T. Ibrahim, B.L. Moctar, K. Tomkouani, D.B. Gbandi, D.K. Victor, N. Phinthè, Kinetics of the adsorption of anionic and cationic dyes in aqueous solution by low-cost activated carbons prepared from sea cake and cotton cake, Am. Chem. Sci. J., 4 (2014) 38–57.
[42] H. Deng, V. Zhang, X. Xu, G. Tao, J. Dai, Optimization of preparation of activated carbon from cotton stalk by microwave assisted phosphoric acid-chemical activation, J. Hazard. Mater., 182 (2010) 217–224.
[43] Q.S. Liu, T. Zheng, N. Li, P. Wang, G. Abulikemu, Modification of bamboo-based activated carbon using microwave radiation and its effects on the adsorption of methylene blue, Appl. Surface Sci., 256 (2010) 3309–3315.
[44] V. Fierro, G. Muñiz, A.H. Basta, H. El-Saied, A. Celzard, Rice straw as precursor of activated carbons: Activation with ortho-phosphoric acid, J. Hazard. Mater., 181(1) (2010) 27–34.
[45] S. Lagergren, About the theory of so called adsorption of soluble substances, K. Sven. Vetensk. akad. Handl., 24 (1898) 1–39.
[46] Y.S. Ho, G. McKay, Sorption of dye from aqueous solution by peat, Chem. Eng. J., 70 (1998) 115–124.
[47] G. Karaçetin, S. Sivrikaya, M. Imamoğlu, Adsorption of methylene blue from aqueous solutions by activated carbon prepared from hazelnut husk using zinc chloride, J. Anal. Appl. Pyrolysis., 110 (2014) 270–276.
[48] Y. Kan, Q. Yue, J. Kong, B. Gao, Q. Li, The application of activated carbon produced from waste printed circuit boards (PCBs) by H_3PO_4 and steam activation for the removal of malachite green, Chem. Eng. J., 260 (2015) 541–549.